PERGAMON

Chemical Engineering Science 56 (2001) 999–1010

Chemical Engineering Science

www.elsevier.nl/locate/ces

Multi-objective optimization of industrial hydrogen plants

J. K. Rajesh[a], S. K. Gupta[b,1], G. P. Rangaiah[a], A. K. Ray[a,*]

[a]*Department of Chemical and Environmental Engineering, National University of Singapore, 10 Kent Ridge Crescent, Singapore 119260, Singapore*
[b]*Department of Chemical Engineering, University of Wisconsin, Madison, WI 53706, USA*

Abstract

Operating hydrogen plants efficiently is a critical issue, central to any energy conservation exercise in petroleum refining and fertilizer industries. To achieve this goal, "optimal" operating conditions for improved unit performance need to be identified. In this work, an entire industrial hydrogen plant is simulated using rigorous process models for the steam reformer and shift converters. An adaptation of the nondominated sorting genetic algorithm (NSGA) is then employed to perform a multi-objective optimization on the unit performance. Simultaneous maximization of product hydrogen and export steam flow rates is considered as the two objective functions for a fixed feed rate of methane to the existing unit. For the specified plant configuration, Pareto-optimal sets of operating conditions are successfully obtained by NSGA for different process conditions. The results serve as a target for the operator to aim at, in order to achieve cost effective operation of hydrogen plants.

Keywords: Steam reforming; Genetic algorithm; Multi-phase reactors; Modeling; Optimization; Systems engineering

1. Introduction

In these days of ever-increasing energy costs and environmental concerns, it is paramount that every chemical process be as energy efficient as possible. The petroleum refining and fertilizer industries are no exceptions to this. In fact, decreasing profit margins and fierce competition have made cost cutting, through efficient and optimal plant operation, inviolable. Of particular interest is the steam reforming process, which is the primary route for producing hydrogen and syngas in the refining and fertilizer industries. The H_2 plant is a highly energy intensive unit, and therefore, one of the most crucial links in the energy conservation chain.

Armor (1999) provided an excellent overview of the significance of hydrogen in the chemical process industry, the present status of hydrogen use and future trends. Recent trends in operating constraints and the environmental legislation have come to affect the process economics of H_2 plants adversely. Shahani, Garodz, Murphy, Baade and Sharma (1998) stressed the need to envisage new strategies to overcome them. They suggested, among others, operating H_2 plants as a source of steam apart from its primary purpose of H_2 production. One of the motivations for the present study is to guide the operator engaged in such an endeavor. Also, the amount of research that has, until now, gone into the optimal operation of H_2 units in entirety, pales in comparison to research on reforming and shift conversion kinetics, and on modeling the corresponding reactors. In an earlier study, our group had successfully optimized the performance of the steam reforming section of an existing H_2 unit (Rajesh, Gupta, Rangaiah & Ray, 2000). In this work, we present an integrated approach to obtain *optimal* steady-state operating conditions for a *complete* industrial H_2 plant, to maximize value addition and minimize running costs simultaneously using an adaptation of genetic algorithm (GA).

A detailed review of relevant literature on the steam reforming process and efforts to model, simulate and optimize reformer performance is available in our earlier study (Rajesh et al., 2000). Notable contributions in the reformer modeling and simulation aspects were made by Singh and Saraf (1979), Xu and Froment (1989a,b) and Elnashaie, Adris, Soliman and Al-Ubaid (1992). Considerable work has also been carried out on the modeling of other major sections in the H_2 unit, namely, the shift converter and the pressure swing adsorption (PSA) unit. The mechanism of shift conversion is a subject of ambiguity even now though it is well known that the reaction takes the chemisorption-surface reaction–desorption

* Corresponding author. Tel.: +65-874-8049; fax: +65-779-1936.
E-mail address: cheakr@nus.edu.sg (A. K. Ray).
[1] On leave from the Indian Institute of Technology, Kanpur, 208016, India.

0009-2509/01/$ - see front matter
PII: S0009-2509(00)00316-X

route. Adsorption isotherms and associated phenomena have however been better understood and modeled.

Elnashaie and Elshishini (1993) have provided a detailed review of past work in the areas of shift conversion kinetics and reactor modeling. Kul'kova and Temkin (1949) proposed the oxidation–reduction mechanism while Oki and Mezaki (1973) proposed a stoichiometric number-based mechanism for the shift conversion reaction. A number of groups have developed kinetic models, which differ to a considerable extent. These conflicting results are believed to be due to the presence of impurities like sulfur in the feed and experimentation under conditions where diffusional resistances are significant.

Boudart (1956) and other researchers put forward power-law rate equations with empirical constants used to fit experimental results. Ruthven (1969) justified considering the reaction as pseudo-first order in CO concentration since steam is in large excess. Singh and Saraf (1977), proceeding on similar lines, derived a rate expression containing factors to account for the effect of temperature, pressure, diffusional resistances, concentration of poisons (H_2S) and the age of the catalyst. Rase (1977) presented a rate expression, which by far, has been the most successful in predicting the kinetics of industrial shift converters. Wolf, Barré-Chassonnery, Höhenberger, van Veen and Baerns (1998) studied the effect of the role of the water-gas shift reaction kinetics on the conversion of methane into syngas in a reformer and found that the lower activation energy of the shift conversion reaction results in a faster reaction rate and a closer approach to equilibrium as compared to steam reforming reactions.

Singh and Saraf (1977) developed a mathematical model for a high-temperature (HT) shift converter based on their kinetic model and verified it by simulating an industrial unit. Elnashaie and Alhabdan (1989) used the kinetic model of Rase (1977) to simulate four cases of industrial HT shift converter operation. They used orthogonal collocation to solve the coupled flux equations with one interior collocation point.

Ahmed, Islam and Ali (1994), using pseudo-first-order kinetics, generated a one-dimensional model for the shift converter. To tune the model, they formulated and solved an optimization problem to minimize the deviation of predicted outlet temperature and conversion from experimental values. Xue, O'Keeffe and Ross (1996) showed that there is a need for operating the shift converter with a low H_2O/CO ratio citing practical considerations. They presented charts that indicated regimes where undesirable side reactions like methanation/coking are possible using thermodynamic calculations.

There have been several studies on the optimization of the shift converter performance in isolation. Hawker (1982) suggested techniques to aid efficient operation of shift converters and to extend the life of the catalyst. Ahmed et al. (1994) used their model to predict an optimal operating strategy for an HT shift converter. They targeted the minimization of CO in the shift converter outlet by changing the inlet temperature, pressure and the steam to gas ratio. Ettouney, Shaban and Nayfeh (1993) performed a theoretical performance analysis of HT and low-temperature (LT) shift converters, and predicted that there exists an optimal HT shift converter feed temperature that results in minimal CO carrying over to the LT shift converter. However, such a unique optimum was not observed with respect to the LT shift converter feed temperature.

PSA modeling and simulation has also had its fair share of interest. Malek (1996) has provided a detailed review of work on modeling and simulation of PSA units used for H_2 separation. Kumar et al. (1994) developed a versatile process simulator to characterize PSA performance using a nonequilibrium, nonisothermal mathematical model. This and other similar efforts involve simulation of PSA units using rigorous, dynamic models. Chlendi, Tondeur and Rolland (1995) obtained correlations to predict H_2 purity and yield as a function of PSA operating parameters. Kumar (1994) suggested techniques to optimize PSA performance through operational changes.

2. Process description

Fig. 1 is a simplified schematic of a typical H_2 plant, which operates on natural gas (predominantly methane) feed. The feed is mixed with appropriate quantities of steam and recycle H_2 before it enters the reforming furnace. An excess of steam (over the stoichiometric ratio) is usually used to further the reforming reactions and to avoid coke formation. A small portion of the product H_2 is recycled back to the feed because H_2 keeps the catalyst in the early part of the reformer tubes (which is H_2 deficient) in its active state. The following important reactions take place within the reformer:

$$CH_4 + H_2O \rightleftharpoons CO + 3H_2, \quad \Delta H_r = 2.061 \times 10^5 \text{ kJ/kmol}, \tag{1}$$

$$CO + H_2O \rightleftharpoons CO_2 + H_2, \quad \Delta H_r = -4.11 \times 10^4 \text{ kJ/kmol}, \tag{2}$$

$$CH_4 + 2H_2O \rightleftharpoons CO_2 + 4H_2, \quad \Delta H_r = 1.650 \times 10^5 \text{ kJ/kmol}. \tag{3}$$

The reforming reactions (1) and (3) occur (in parallel) primarily in the steam reformer while thermodynamics favor higher conversions of the shift conversion reaction (2) in the shift reactors. The hot syngas at the reformer outlet is cooled in E1 (Fig. 1) before it enters the HT shift converter. In E1, the syngas exchanges thermal energy with boiler feed water (BFW) to generate very high-pressure steam. Inside the HT shift converter the

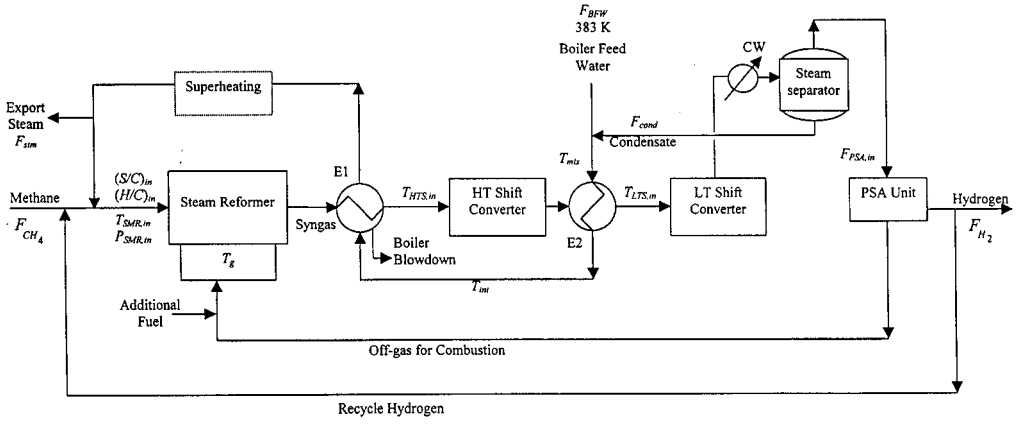

Fig. 1. Simplified process flow diagram for H_2 production by steam reforming of methane.

exothermic reaction (2) occurs predominantly resulting in additional H_2 production and an increase in gas temperature. The process gas is again cooled in E2, this time its thermal energy being used to preheat BFW. The process gas then reacts further in the LT shift converter. The H_2-rich exit stream from the LT shift converter is cooled and then flashed to remove the excess steam as condensate (which is recycled back into the process). The H_2-rich stream devoid of most of its water content goes to the PSA unit for separation of H_2 from the off-gas. The PSA off-gas along with additional fuel is used for combustion in the reformer furnace. The steam generated is used for mixing with the feed (internal use) as well as for "export" outside the unit (Fig. 1).

3. Mathematical model and simulation

Considering that many H_2 units are already in operation in the world, this study considers modeling and optimization of an existing industrial H_2 plant. Therefore, its operation is influenced by design limitations, kinetic, thermodynamic and other physico-chemical considerations. Our aim is to explore the possibility of operating such a H_2 plant so as to maximize the value addition per unit feed processed with only very minor equipment modifications. However, the findings of this study will also be useful for the design of new H_2 plants.

The steam reformer model used in the present study is identical to the one reported by Rajesh et al. (2000). Since the mathematical model and simulation of the reformer are described there in detail, the same are not included here for brevity. However, it is to be noted that extent of the reforming reactions is controlled largely by the rate of heat transfer from the furnace to the catalyst pellet and reacting gases inside the reformer tubes, and also the severe diffusional resistances within the porous catalyst pellets. The HT/LT shift converter model and parameter values used are similar to that of Elnashaie and Alhabdan (1989). Only the reactor dimensions were modified to maintain the same space velocity for the current operating throughput based on reformer design. Therefore, only the basic equations are provided in Appendix 1, and the reader is referred to Elnashaie and Alhabdan (1989) for further details. Since the steam generation system is integrated with the process, an energy balance is performed to estimate the heat duty of exchangers ($E1$ and $E2$) and thereby calculate the quantity of steam produced iteratively.

The steam separator was modeled as an isothermal flash of the process gas that is cooled to room temperature. The PSA unit was simulated as a "black box" with a 90% H_2 recovery and 99.95% H_2 purity in the product. This is justified for the following reasons. Optimization of an existing H_2 plant considered in this study is likely to result in changes in the inlet stream to the PSA unit. The study of Chlendi et al. (1995) indicates that critical performance criteria like H_2 yield and purity are largely insensitive to nominal changes in PSA feed composition and pressure that are possible among the various normal operating scenarios. If necessary, required H_2 yield and purity can be achieved by minor modifications to adsorption/desorption cycle times, which are shown by Chlendi et al. (1995) to have greater effect on the performance of a PSA unit. A summary of the model equations used for the steam separator and PSA unit, is also included in the Appendix.

The steady-state model equations for the entire system were solved on a CRAY J916 supercomputer using the mathematical routines available in IMSL. One complete simulation of the H_2 unit required 2 seconds of CPU time on the CRAY J916. The results obtained from the simulation of the steam reformer were found to match plant data (Rajesh et al. 2000). The model for the shift converters was verified by comparing simulation results against published industrial data (Elnashaie & Elshishini,

1993). The integrated model was found to be reliable and accurate in characterizing the physical processes occurring and therefore, considered suitable for use in the envisaged optimization study.

4. Formulation of the optimization problem

The optimization problem is solved for a fixed feed rate of methane, F_{CH_4}, to the unit. The profitability of operating an existing H_2 plant under this condition is dictated *essentially* by the value of the product H_2 and the price that the export steam can fetch. It is, therefore, logical to search for operating scenarios that will maximize flow rates of both product H_2, F_{H_2}, and export steam, F_{stm}, simultaneously. Performing a constrained multiobjective optimization with both of them as objectives can identify such scenarios. Expressed mathematically, the optimization problem would be

$$\text{Maximize} \quad J_1 = F_{H_2}, \tag{4}$$

$$J_2 = F_{stm}, \tag{5}$$

subject to

$$T_{w,o} \leqslant 1200 \text{ K}, \tag{6}$$

$$\left[\frac{y_{H_2O}}{y_{H_2}}\right]_{HTS} \geqslant 0.3, \tag{7}$$

$$T_{LTS} \geqslant (T_{dew} + 15) \text{ K}, \tag{8}$$

$$Q_{E_i} \leqslant 1.2 \times Q_{E_i\,max}, \quad i = 1, 2, \tag{9}$$

$$F \leqslant 1.2 \times F_{max} \tag{10}$$

and the model equations for the system given in Appendix 1. Srinivas and Deb (1995) have shown that the maximization of a function J, can be replaced by the minimization of a function I, where $I = [1/(1 + J)]$, without the transformation changing the location of the optima. If $J \neq 0$, the function I may be simplified as $I = [1/J]$.

The constraint on the outer wall temperature, $T_{w,o}$, of the reformer tube (Eq. (6)) is based on the creep limit of alloy steel tubes at operating conditions and is required to avoid the rupture/creep of tubes. The (H_2O/H_2) molar ratio (Eq. (7)) should be above 0.3 at any location in the HTS to ensure that methanation reactions do not occur within this reactor. Also, the operating temperature of the process gas at any position within the LTS should be maintained at least 15°C above the dew point of the bulk gas to avoid the risk of steam condensing within the catalyst pores (which leads to catalyst deactivation). Constraints are also required to keep the heat duties of the two exchangers downstream of the reformer, and the total unit feed rate (inclusive of the recycle streams) within design margins (Eqs. (9) and (10)). This is to ensure that the operation at the optimal conditions is feasible using the existing equipment without the need for design modifications.

Seven decision variables were selected for solving the optimization problem. It is well known that the performance of the reformer influences that of the entire H_2 unit to a great extent. Specifying gas temperature ($T_{SMR,in}$), pressure ($P_{SMR,in}$), furnace gas temperature (T_g), the gas composition and flow rate at reformer inlet fixes the heat input to the process gas and thereby the extent of conversion. This is because the endothermic reforming reactions proceed close to thermodynamic equilibrium, particularly in the later section of the reformer. The shift converters are fixed-bed adiabatic reactors which, for a given gas composition, have only one degree of operational freedom — the inlet temperature. Therefore, fixing $T_{HTS,in}$ and $T_{LTS,in}$ specifies the state of the system completely. The following bounds are used for the decision variables based on industrial practice:

$$725 \leqslant T_{SMR,in} \leqslant 900 \text{ K}, \tag{11a}$$

$$2450 \leqslant P_{SMR,in} \leqslant 2950 \text{ kPa}, \tag{11b}$$

$$2.0 \leqslant (S/C)_{in} \leqslant 6.0, \tag{11c}$$

$$0.0 < (H/C)_{in} \leqslant 0.5, \tag{11d}$$

$$1375 \leqslant T_g \leqslant 1675 \text{ K}, \tag{11e}$$

$$570 \leqslant T_{HTS,in} \leqslant 730 \text{ K}, \tag{11f}$$

$$400 \leqslant T_{LTS,in} \leqslant 530 \text{ K}. \tag{11g}$$

The lower limit on $T_{SMR,in}$ is decided by thermodynamic limitations to prevent gum formation on the reformer catalyst. The upper limit on $T_{SMR,in}$ is based on the maximum heat that the feed can normally pick up from the flue gases in the convection section of industrial reforming furnaces. The minimum and the maximum values of $P_{SMR,in}$, have been selected, respectively, based on the normal pressure at which H_2 is to be produced in the plant and the supply pressure of the natural gas feed. The lower limit of $(S/C)_{in}$ is set at 2.0 to avoid carbon formation on the catalyst, which could occur at lower values. Very high $(S/C)_{in}$ affects the process economics adversely because it involves the heating of the excess steam up to reforming (outlet) temperature and subsequent condensation downstream of the reformer. The maximum $(S/C)_{in}$ is usually limited to 6.0 based on industrial practice. The maximum value of $(H/C)_{in}$ is limited to 0.5 to avoid unnecessary recycle of H_2 to the reformer. While performing the optimization, the bounds specified in Eq. (11c) were modified based on the choice of the other decision variables as described in Rajesh et al. (2000). Bounds on T_g, $T_{HTS,in}$ and $T_{LTS,in}$ have been fixed based on normal operating ranges in industrial units. The LT shift catalyst is temperature sensitive and should not be exposed to high temperature, which results in irreparable damage to the catalyst.

The performance constraints defined in Eqs. (6)–(10) were combined into the objective functions in the form of penalty functions. The method involved penalizing the objective function in proportion to the extent of constraint violation (i.e., the penalty function takes a finite value when a constraint is violated and a value of zero if the constraint is satisfied). The objective functions considered for minimization, finally, are thus,

$$I_1 = \frac{1}{F_{H_2}} + 10^4 \sum_{i=1}^{6} f_i, \tag{12}$$

$$I_2 = \frac{1}{F_{stm}} + 10^4 \sum_{i=1}^{6} f_i, \tag{13}$$

where

$$f_1 = (T_{w,0} - 1200) + |(T_{w,0} - 1200)|,$$

$$f_2 = \left[\frac{y_{H_2O}}{y_{H_2}} - 0.3\right] - \left|\left[\frac{y_{H_2O}}{y_{H_2}} - 0.3\right]\right|,$$

$$f_3 = [T - (T_{dew} + 15)] - |[T - (T_{dew} + 15)]|,$$

$$f_4 = (Q_{E1} - 1.2Q_{E1max}) + |(Q_{E1} - 1.2Q_{E1max})|,$$

$$f_5 = (Q_{E2} - 1.2Q_{E2max}) + |(Q_{E2} - 1.2Q_{E2max})|,$$

$$f_6 = (F - 1.2F_{max}) + |(F - 1.2F_{max})|.$$

The optimization problem described above is solved using an adapted version of genetic algorithm suitable for multi-objective problems, referred to as the non-dominated sorting genetic algorithm (NSGA). More details about this algorithm are available in Srinivas and Deb (1995). Recently, applications of multiobjective optimization in chemical engineering has been reviewed by Bhaskar, Gupta and Ray (2000).

5. Results and discussion

The optimization problem involves two objective functions, which are influenced in opposite directions by changes in some of the decision variables. Table 1 shows the effect of variation in the decision variables on the objective functions considered. It has been generated based on a parametric sensitivity analysis of the simulated mathematical model of the system as briefly discussed below.

The reforming reactions are inhibited at high P_{in} while shift conversion is unaffected by variations in P_{in}. Therefore, the production of both H_2 and steam is improved by operating the unit at as low a P_{in} as possible. The endothermic reforming reactions are favoured when the operating temperature within the reformer is high (achievable with a high $T_{SMR,in}$ and T_g), while the exothermic shift conversion reaction is favoured when the temperature inside the shift converters is low (implying low $T_{HTS,in}$ and $T_{LTS,in}$). The maximum value of the outer tube wall temperature, $T_{w,0}$, (as fixed in Eq. (6)) limits the maximum possible exit temperature of the process gas, which in turn, influences the extent of the reforming and shift conversion reactions and hence, the objective functions. Operating the reformer at as high a temperature and the shift converters at as low a temperature as possible therefore helps both objective functions: It increases H_2 production and also makes more heat available for steam generation in E1. Hence, it is clear that changes in decision variables $P_{SMR,in}$, $T_{SMR,in}$, T_g, $T_{HTS,in}$ and $T_{LTS,in}$ influence H_2 and steam production in the same manner.

Table 1
Effect of an increase in the decision variable on the objective functions

Objective function	Effect of Increase in						
	$T_{SMR,in}$	$P_{SMR,in}$	$(H/C)_{in}$	$(S/C)_{in}$	T_g	$T_{HTS,in}$	$T_{LTS,in}$
F_{H_2}	↑	↓	↓	↑	↑	↓	↓
F_{stm}	↑	↓	↑	↓	↑	↓	↓

From an analysis of the model (and Le'Chatelier's principle) it can also be observed that excess steam in the feed would favor all the forward reactions (1)–(3) leading to more H_2 production through higher conversions of methane. However, more steam in the feed also results in reaction (3) dominating over reaction (1), producing more CO_2 (and less CO). This reduces the extent of exothermic reaction (2) taking place in the shift converter and reduces steam generation. Similarly, large amounts of recycle H_2 will inhibit reaction (3) and, to a lesser extent, reactions (1) and (2). This will reduce CH_4 conversion and H_2 production, but will increase CO formation and result in more steam being generated. Therefore, H_2 production is favoured at low $(H/C)_{in}$ and high $(S/C)_{in}$, while more export steam will be available at high $(S/C)_{in}$ and low $(H/C)_{in}$. This conflict between the effects of the decision variables on the objective functions, results in the optimum being a Pareto-optimal set rather than a unique solution. A Pareto set (for the present case of two objective functions) has the property that when we move from any one point on the set to another, one objective function improves but the other worsens. Hence, neither solution "dominates" over the other, and both are equally good. One has to use the additional information that is often intuitive (based on experience) and nonquantifiable in nature, to choose an operating point (preferred solution) from among the entire Pareto set, for operation. In other words, it is not possible to identify a unique set of operating conditions that will maximize both H_2 and steam production rates.

Fig. 2 shows the Pareto set of optimal solutions obtained for the problem formulated above. The values of F_{H_2} and F_{stm} are plotted rather than those of I_1 and

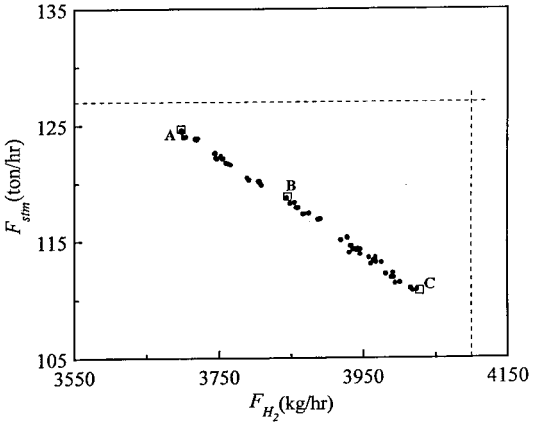

Fig. 2. Pareto-optimal set of solutions obtained for the simultaneous optimization of F_{H_2} and F_{stm}.

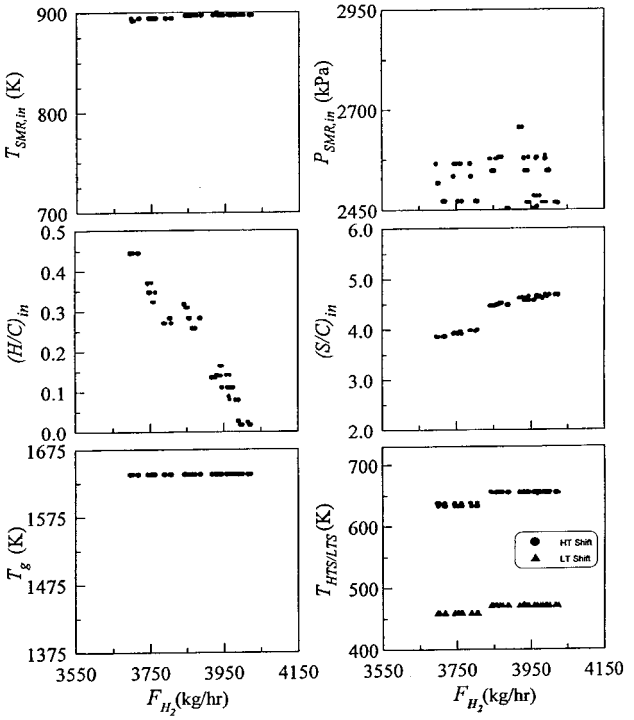

Fig. 3. Decision variables corresponding to each of the Pareto-optimal solutions shown in Fig. 2.

I_2 since the penalty functions have no contribution to the objective functions on attainment of convergence. Plotting the physical objectives directly rather than the actual objective function gives the operator a better perspective when he/she is required to choose or discriminate among the various operating scenarios. The dotted lines in the Pareto set (Fig. 2) indicate the maximum possible H_2 or steam production rate with the given operating constraints, obtained by solving two single objective optimization problems (either Eq. (12) or (13)). The benefit of a multi-objective optimization is evident upon observing the wide choice of operating points available in the Pareto-optimal set; by using conventional techniques we would have been able to predict only 2 optimal solutions (corresponding to the intersection of the curve in Fig. 2 with the two dotted lines). The CPU time taken to generate one set of Pareto-optimal solutions (such as those in Fig. 2) is 24 min on the CRAY J916. Although a super computer was used in this study, it may be possible to carry out the multi-objective optimization of the H_2 unit on the latest personal computers.

Each point (referred to as a chromosome) on the Pareto set (Fig. 2) is associated with a set of decision variables. Fig. 3 is a plot of the decision variables corresponding to each of the points on the Pareto set. To obtain the operating conditions for a desired hydrogen production rate (and a corresponding steam generation rate from Fig. 2), one has to read off from Fig. 3, the values of the decision variables corresponding to the desired abscissa value. It is consistent with our parametric analysis in Table 1. From Fig. 3, we observe that $(S/C)_{in}$ and $(H/C)_{in}$, as expected, have opposing trends with respect to F_{H_2} (and F_{stm} also). As predicted, all the decision variables other than $(S/C)_{in}$ and $(H/C)_{in}$ converge to a nearly constant value since they affect both the objectives in a similar manner. This confirms our expectation that it is possible to find a single value of each of these parameters (close to one of their bounds) that maximizes both objective functions. Such a unique value does not exist for $(S/C)_{in}$ and $(H/C)_{in}$.

It is to be noted that these optimal values depend on the specified methane feed rate and maximum allowable tube wall temperature, which are subject to change over the short- and log-term operation of the unit. By performing optimization with respect to $(S/C)_{in}$ and $(H/C)_{in}$ only, one would be unable to obtain optimal values of the other five decision variables for every new operating scenario. Inclusion of all the seven decision variables in the optimization, as in the present study, provides extra degrees of freedom resulting in superior solutions. It was observed that the effect of $P_{SMR,in}$ on the objective functions was very mild, as evidenced by the scatter in its optimal values in Fig. 3.

Table 2 lists values of the decision variables corresponding to three chromosomes, A, B and C selected from the Pareto set in Fig. 2. From this table, it is apparent that there is a trade-off between maximizing hydrogen and steam production rates. The external fuel requirement, $F_{ext\ fuel}$, (which is the difference between the reformer fired duty and the energy available from PSA off gases) is also shown for each of these cases. The knowledge of the costs of hydrogen, steam and external fuel will enable one to choose a single solution from among all the possible solutions that will yield maximum profit.

Table 2
Comparison of operating parameters for three possible cases of optimal operation for a fixed natural gas feed rate, $F_{CH_4,in} = 709.3$ kmol/h

Parameter	Chromosome A	Chromosome B	Chromosome C
$T_{SMR,in}$ (K)	893.5	896.6	896.7
$P_{SMR,in}$ (kPa)	2563.3	2576.3	2466.0
$(H/C)_{in}$	0.444	0.316	0.0157
$(S/C)_{in}$	3.86	4.45	4.67
T_f (K)	1637.1	1637.5	1637.5
T_{HTS} (K)	635.7	654.6	653.3
T_{LTS} (K)	457.6	470.1	470.1
F_{H_2} (kg/h)	3697	3844	4025
F_{stm} (ton/h)	124.50	118.70	110.80
$Q_{ext\,fuel}$ (Gcal/h)	58.91	64.07	69.38

Figs. 4 and 5 show the conversion and temperature profiles while operating the H_2 unit under the conditions detailed in Table 2. The conversions of CH_4, CO_2 and CO at the reactor outlet (which can be obtained from Fig. 4) for the three operating cases (decision variables for which are given in Table 2), essentially confirms the findings of the parametric sensitivity study summarized in Table 1. The optimized profiles in Fig. 5 indicate that the tube outer wall temperature is near its upper limit (1200 K) at the outlet of the reformer, in line with the earlier intuitive analysis and normal industrial practice of operating reformers in H_2 units close to the highest allowable temperature. The variation of each of the component mole fractions along the length of the reformer and shift converters corresponding to chromosome A is shown in Fig. 6. Profiles for chromosomes B and C are similar.

Fig. 7 shows the variation of the Pareto-optimal set with changes in F_{CH_4}. We observe a diagonal shift of the Pareto-optimal set with a change in F_{CH_4}. This is expected since higher F_{CH_4} can give more F_{H_2} and also generate more F_{stm}. The latter is because of the higher amount of recoverable energy in the process gas at the reformer outlet. An engineer can choose from among the optimal operating points in Fig. 7 corresponding to a desired hydrogen or steam production rate. Such a feature allows him/her to reset operating conditions to new optimal values based on the latest processing and market constraints. Table 3 gives the process conditions and outcomes for two possible operating points for each of these scenarios.

The sensitivity of the Pareto to the operational constraint on the maximum allowable tube (outer) wall temperature is shown in Fig. 8. It follows from the earlier discussion that higher tube wall temperatures allow higher conversions of methane resulting in higher F_{H_2} and higher F_{stm}. This is borne out by the observed shift of the Pareto. This shift is of practical significance because reformers are operated such that the maximum possible tube wall temperature decreases as the tube ages. Fig. 8 can therefore be used to change the operating point of a reformer with the life of the tubes — an exercise that

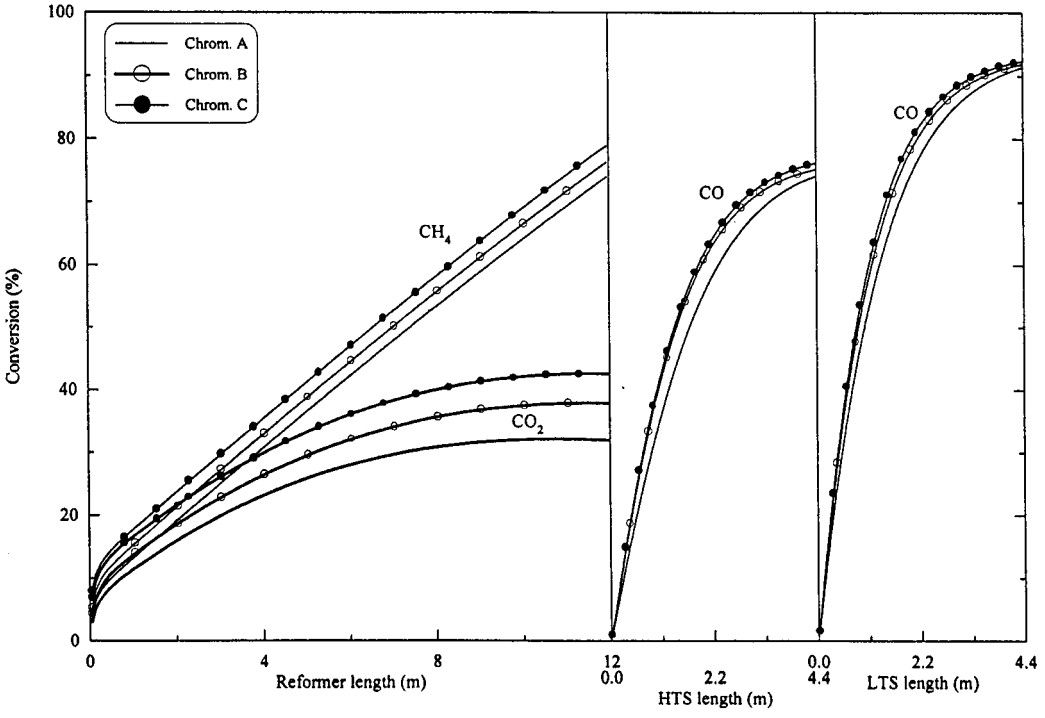

Fig. 4. Conversion profiles of CH_4 and CO_2 in the reformer, and of CO in the HT and LT shift converters for each of the three chromosomes A, B and C.

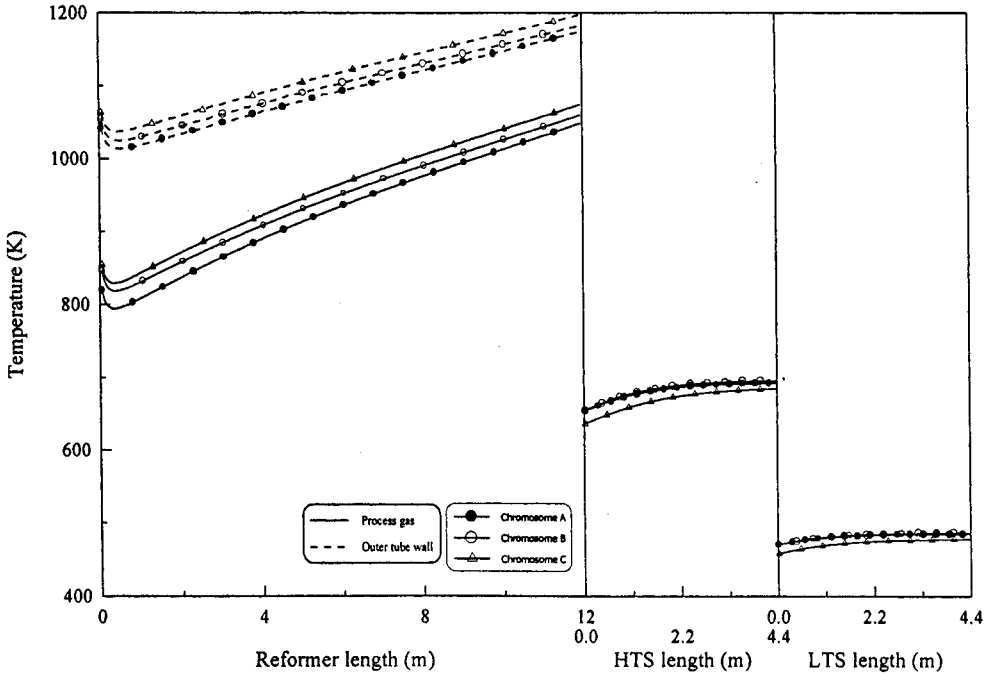

Fig. 5. Process gas and reformer tube wall temperature profiles for each of the three chromosomes A, B and C.

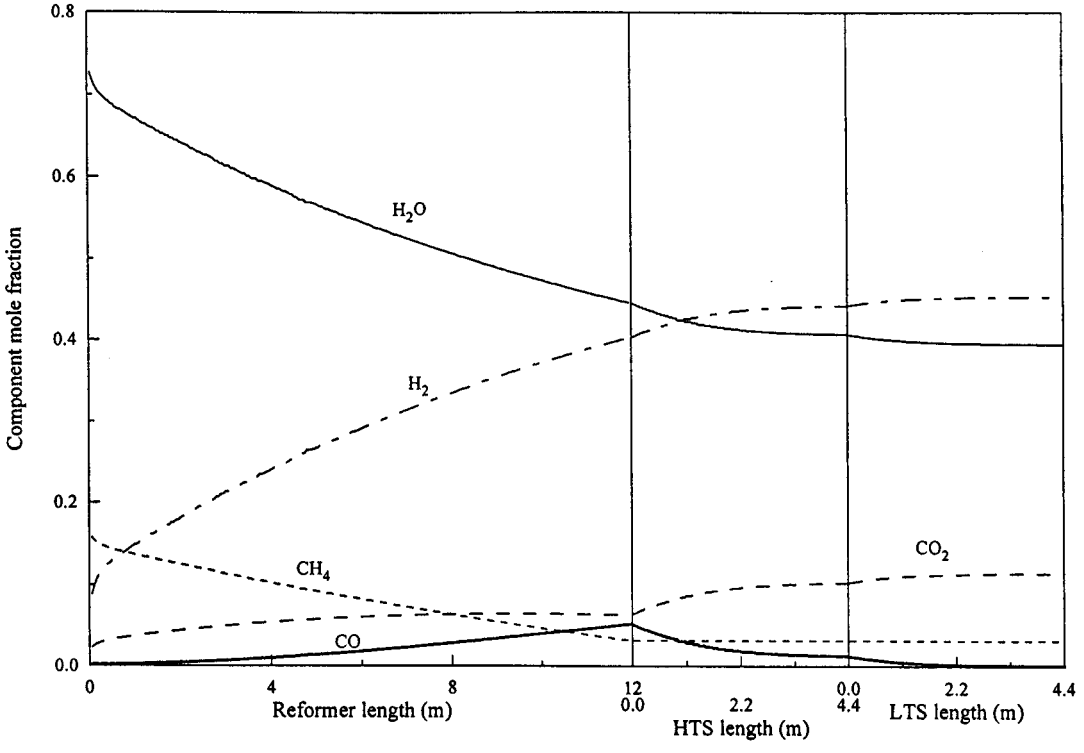

Fig. 6. Composition profile of reacting components for operation of the H_2 unit at conditions corresponding to chromosome A.

otherwise requires many years of operating experience to establish.

The above results in Figs. 2–8 and Tables 2 and 3 on the multi-objective optimization of the H_2 unit for a range of conditions, were successfully obtained using NSGA, which is a nontraditional search and optimization technique that mimics the principles of genetics and natural selection (i.e., survival of the fittest). The

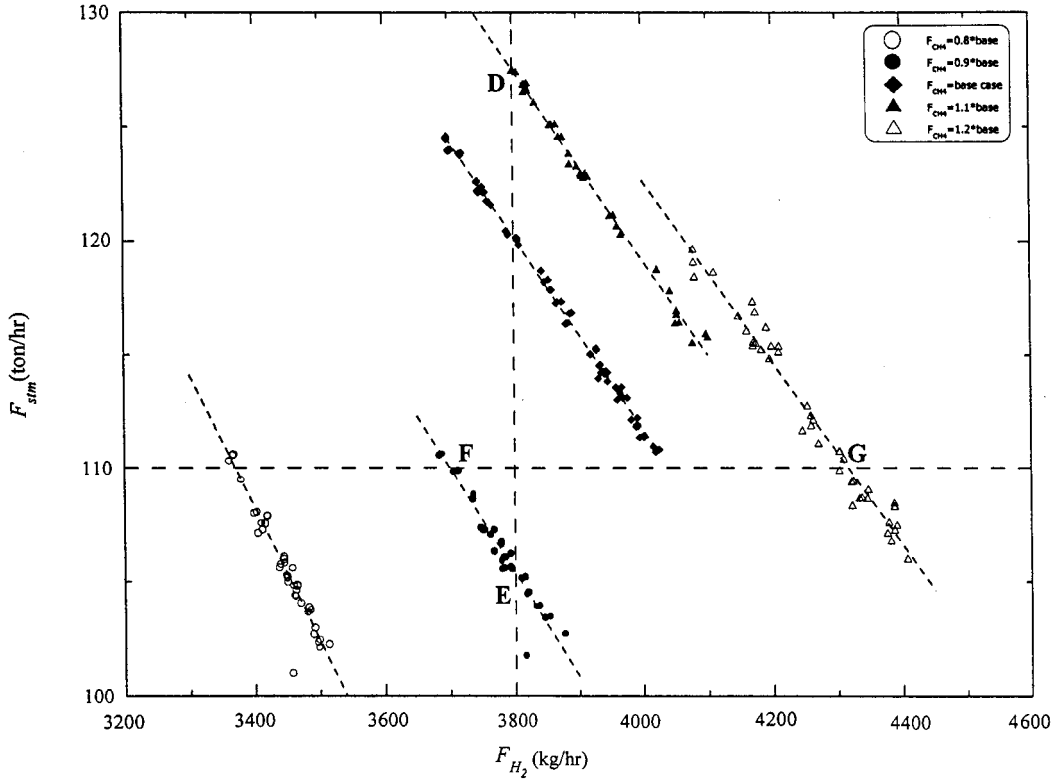

Fig. 7. Nomograph for the variation of the H_2 production and steam generation due to change in methane feed rate.

Table 3
Comparison of operating parameters for two possible cases of optimal operation for a fixed hydrogen production rate F_{H_2}, and for a fixed export steam generation rate F_{stm}

Case	$F_{H_2} \approx 3800$ kg/h		$F_{stm} \approx 110$ ton/h	
Parameter	Chrom. D	Chrom. E	Chrom. F	Chrom. G
$T_{SMR,in}$ (K)	894.2	899.8	896.5	896.4
$P_{SMR,in}$ (kPa)	2669.5	2506.1	2466.3	2882.7
$(H/C)_{in}$	0.422	0.391	0.477	0.089
$(S/C)_{in}$	3.47	5.44	5.47	3.897
T_f (K)	1646.6	1636.7	1599.8	1672.6
$T_{HTS,in}$ (K)	655.8	691.4	636.4	696.4
$T_{LTS,in,}$ (K)	465.2	511.8	465.5	525.5
$F_{CH_4,in}$ (kmol/h)	780.2	638.4	567.4	851.2
F_{H_2} (kg/h)	3801.3	3794.8	3361.4	4302.1
F_{stm} (ton/h)	127.46	105.53	110.29	109.84
$Q_{ext\,fuel}$ (Gcal/h)	50.93	76.41	68.71	58.69

algorithm preferentially chooses the "fitter" solutions (those which give lower objective function values) for subsequent GA operations (mutation and crossover). Each round of iterative progress towards the minimum is termed as one generation. The evolution of the Pareto optimal solution set shown in Fig. 2, with number of generations is shown in Fig. 9. The convergence of solutions from the initial randomness to the final smooth shape can be observed. The solutions were found to be insensitive to changes in the values of the major NSGA parameters employed, values of which are indicated in Table 4.

Once the Pareto set is obtained, an engineer can choose to operate the reformer at the set of operating conditions corresponding to any one of the Pareto points using his operating experience, judgment or other information that has not been incorporated while generating the optimal solutions (e.g., economic considerations). A single point on the Pareto (referred to as the preferred solution) is usually chosen for operation. This point is often arrived at by having several plant personnel rate the Pareto points according to their preferences and then taking a weighted average of their choices. While performing such an exercise, knowledge about the reformer heat duty that has to be met by external fuel will be valuable. Note that this heat duty can easily be calculated using the results from the multi-objective optimization; see the last entry in Tables 2 and 3.

6. Conclusions

The present work addresses the real-life challenge of enhancing value addition in industrial H_2 generation

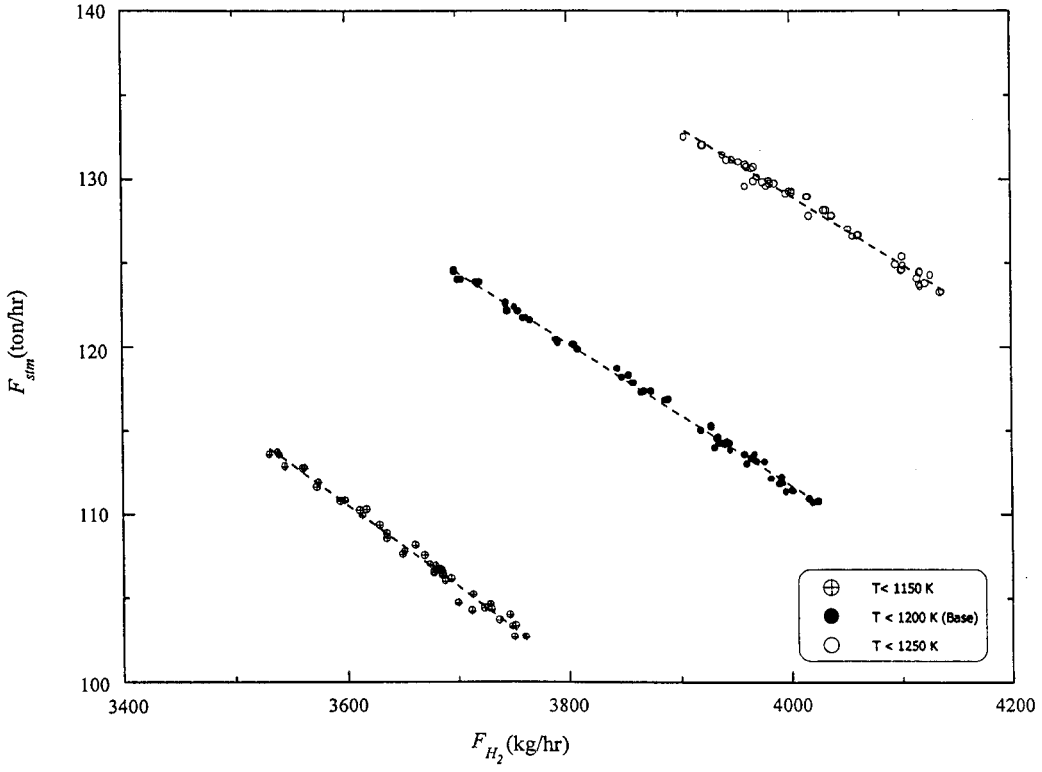

Fig. 8. Nomograph for the variation of the H_2 production and steam generation due to change in furnace tube wall constraint.

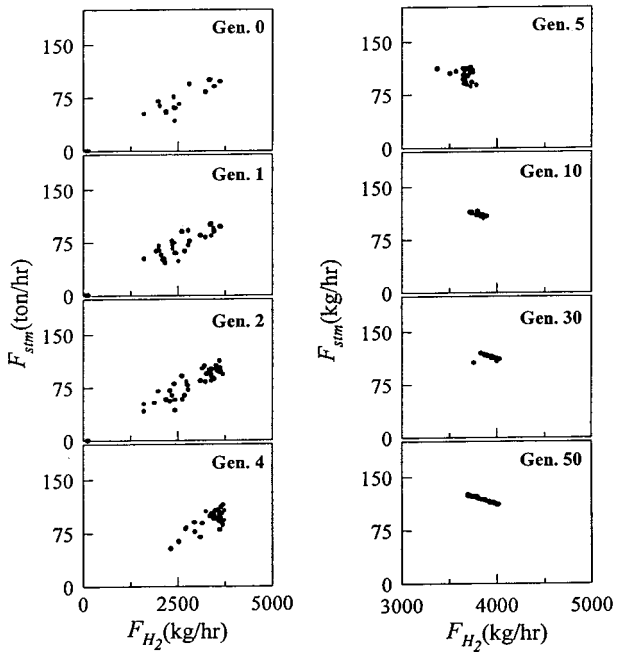

Fig. 9. Evolution of the Pareto set with increase in number of generations.

plants at steady state conditions. Prediction of optimal operating conditions for these units is difficult in view of the large number of decision variables with complex interdependencies. In this study, the value addition is achieved by maximizing the production rate of steam that is exported from the unit in addition to maximizing H_2 production rate for a given feed rate. By performing a multi-objective optimization using the NSGA technique, the plant operator is provided with, not one, but many sets of operating conditions that will yield such an end result.

The significance of the study is that it presents him/her with nomographs, which can be used to quickly arrive at optimal operating parameters for various operational targets. In addition, these nomographs can be customized based on unit-specific constraints. Valuable information like the amount of external fuel requirement for each case of operation is also available allowing the engineer to make an intelligent choice among the various

Table 4
NSGA parameters and their values

Parameter	Value
Population size	50
No. of generations	50
Length of chromosome	24 bits
Crossover probability	0.70–0.75
Mutation probability	0.001–0.002
Spreading parameter, α	2.0
Spreading parameter, σ	0.05

operating points. Operation under the conditions predicted will reduce plant operating costs, enhance productivity and thereby increase profits.

Notation

C_p specific heat of process gas, kcal/kmol/K
$\bar{C}_p$ average specific heat of process gas, kcal/kmol/K
d_i internal diameter of the shift converter, m
F total molar feed rate, kmol/h
F_i molar flow rate of component i at any axial location in the reactor, kmol/h
F_{stm} flow rate of export steam, ton/h
F_{H_2} flow rate of hydrogen from the unit, kg/h
H_{PSA} recovery of H_2 in the PSA unit
$(H/C)_{\text{in}}$ recycle hydrogen/methane molar ratio in the feed
J_{SS} steam separator operating efficiency
l axial location in the shift converter, m
L total length of the shift converter bed, m
P operating pressure at any location, kPa
Q heat duty, kcal/h
r_{CO} rate of reaction of CO on the catalyst surface at any axial location, kmol/h/kg catalyst
S_{PSA} purity of H_2 product from the PSA unit
$(S/C)_{\text{in}}$ steam/methane molar ratio in the feed
T proces gas temperature at any axial location in the reactor, K
$T_{w,o}$ temperature of the outer tube wall, K
x_i conversion of component i at any axial location within the reactor, $i = \text{CH}_4$, CO
x_{CO_2} conversion of CO_2 at any axial location within the reformer defined as $x_{\text{CO}_2} = (F_{\text{CO}_2} - F_{\text{CO}_2,\text{in}})/F_{\text{CH}_4,\text{in}}$
y_i mole fraction of the component i in the bulk gas at any axial location

Greek symbols

$(-\Delta H_r)$ heat of the reaction, kcal/kmol
Ψ activity factor for shift converter catalyst

Subscripts

BFW boiler feed water
cond recycle condensate
$E1$ steam generator
$E2$ preheater for BFW
ext fuel external fuel
HTS HT shift converter
in at the inlet to the section
int intermediate
LTS LT shift converter
mix combined stream of BFW and recycle condensate
out at the outlet of the section
PSA pressure Swing Adsorption Unit
SMR steam reformer
stm steam
SS steam separator

Appendix A. Model equations used for H_2 plant optimization

Steam reformer: Please refer Rajesh et al. (2000) for the model equations.

Shift converter:

$$\frac{\mathrm{d}x_{\text{CO}}}{\mathrm{d}l} = \frac{\pi d_i^2}{4} \times \frac{r_{\text{CO}}}{F_{\text{in}}}, \quad x_{\text{CO}} = 0 \quad \text{at } l = 0, \tag{A.1}$$

$$\frac{\mathrm{d}T}{\mathrm{d}l} = \frac{-\Delta H_r}{C_p} \times \frac{\pi d_i^2}{4} \frac{r_{\text{CO}}}{F_{\text{in}}}, \quad T = T_{\text{in}} \quad \text{at } l = 0. \tag{A.2}$$

For HT shift converter

$$r_{\text{CO}} = 0.0423 \Psi_{\text{HTS}} \exp\left\{15.95 - \frac{4900}{T}\right\} \left[y_{\text{CO}} y_{\text{H}_2\text{O}} - \frac{y_{\text{H}_2} y_{\text{CO}_2}}{\exp(-4.33 + 4900/T)}\right]. \tag{A.3}$$

For LT shift converter

$$r_{\text{CO}} = 0.0423 \Psi_{\text{LTS}} \exp\left\{12.88 - \frac{1855.5}{T}\right\} \left[y_{\text{CO}} y_{\text{H}_2\text{O}} - \frac{y_{\text{H}_2} y_{\text{CO}_2}}{\exp(-4.33 + 4577.778/T)}\right], \tag{A.4}$$

$$y_{\text{CO}} = y_{\text{CO,in}}(1 - x_{\text{CO}}), \tag{A.5}$$

$$y_{\text{H}_2\text{O}} = y_{\text{H}_2\text{O,in}} - y_{\text{CO,in}} x_{\text{CO}}, \tag{A.6}$$

$$y_{\text{CO}_2} = y_{\text{CO}_2,\text{in}} + y_{\text{CO,in}} x_{\text{CO}}, \tag{A.7}$$

$$y_{\text{H}_2} = y_{\text{H}_2,\text{in}} + y_{\text{CO,in}} x_{\text{CO}}. \tag{A.8}$$

Please refer Elnashaie and Alhabdan (1989) for parameter values.

Steam generation system: F_{stm} is calculated by eliminating T_{int} from the following:

Energy balance across E1:

$$(F_{\text{BFW}} + F_{\text{cond}}) C_{p,\text{BFW}} (516 - T_{\text{int}}) + \left\{\frac{F_{\text{BFW}}}{1.05} + F_{\text{cond}}\right\} \lambda_{\text{BFW}} = Q_{E1} = F_{\text{SMRout}} \bar{C}_p (T_{\text{SMRout}} - T_{\text{HTSin}}) \tag{A.9}$$

and energy balance across E2:

$$(F_{\text{BFW}} + F_{\text{cond}}) C_{p,\text{BFW}} (T_{\text{int}} - T_{\text{mix}}) = Q_{E2} = F_{\text{HTSout}} \bar{C}_p (T_{\text{HTSout}} - T_{\text{LTSin}}), \tag{A.10}$$

where F_{BFW} (which includes provision for a blowdown of 5% from the steam generator) is computed as

$$F_{\text{BFW}} = 1.05[F_{\text{stm}} + 2F_{\text{CH}_4\text{in}}(1 - x_{\text{CH}_4,\text{SMRout}})] \tag{A.11}$$

and

$$F_{\text{cond}} = F_{\text{LTSout}}[(1 - J_{SS})y_{\text{H}_2\text{O,LTSout}}] \simeq F_{\text{CH}_4\text{in}}[(S/C)_{\text{in}} - 2(1 - x_{\text{CH}_4,\text{SMRout}})], \quad \text{(A.12)}$$

$$T_{\text{mix}} = \left(\frac{383F_{\text{BFW}} + F_{\text{cond}} \times T_{SS}}{F_{\text{BFW}} + F_{\text{cond}}}\right). \quad \text{(A.13)}$$

Steam separator:

$$F_{SS,\text{out}} = F_{\text{PSAin}} = F_{\text{LTSout}}[1 - (1 - J_{SS})y_{\text{H}_2\text{O,LTSout}}], \quad \text{(A.14)}$$

$$y_{\text{H}_2\text{O},SS\text{out}} = y_{\text{H}_2\text{O,PSAin}} = J_{SS} \times y_{\text{H}_2\text{O,LTSout}}, \quad \text{(A.15)}$$

where J_{SS} is calculated assuming an isothermal flash as

$$J_{SS} = \left(\frac{T_{SS} - 273}{100}\right)^4 \times \frac{101.652}{P_{SS} \times y_{\text{H}_2\text{O,LTSout}}}. \quad \text{(A.16)}$$

PSA unit:

$$F_{\text{H}_2} = y_{\text{H}_2,\text{PSAout}} \times F_{\text{PSAout}}, \quad \text{(A.17)}$$

where

$$y_{\text{H}_2,\text{PSAout}} = S_{\text{PSA}}, \quad \text{(A.18)}$$

$$y_{i,\text{PSAout}} = (1 - S_{\text{PSA}}) \times \frac{y_{i,\text{PSAin}}}{\sum y_{i,\text{PSAin}}}, \quad i = \text{CH}_4,\ \text{H}_2\text{O},\ \text{CO},\ \text{CO}_2,\ \text{N}_2, \quad \text{(A.19)}$$

$$F_{\text{PSAout}} = H_{\text{PSA}} \times \left(\frac{y_{\text{H}_2,\text{PSAin}}}{S_{\text{PSA}}}\right) F_{\text{PSAin}}. \quad \text{(A.20)}$$

References

Ahmed, K., Islam, K. A., & Ali, S. (1994). An optimal operating policy for high temperature shift converters. *Transactions of the Institute of Chemical Engineers, Part A*, *72*, 645–650.

Armor, J. N. (1999). The multiple roles for catalysis in the production of H_2. *Applied Catalysis A: General*, *176*, 159–176.

Bhaskar, V., Gupta, S. K., & Ray, A. K. (2000). Applications of multiobjective optimization in chemical engineering. *Reviews in Chemical Engineering*, *16*(1), 1–54.

Boudart, M. (1956). Kinetics on ideal and real surfaces. *American Institute of Chemical Engineers Journal*, *2*, 62–69.

Chlendi, M., Tondeur, D., & Rolland, F. (1995). Method to obtain a compact representation of process performances from a numerical simulator: Example of pressure swing adsorption for pure hydrogen production. *Gas Separation and Purification*, *9*, 125–135.

Elnashaie, S. S. E. H., Adris, A. M., Soliman, M. A., & Al-Ubaid, A. S. (1992). Digital simulation of industrial steam reformers for natural gas using heterogeneous models. *Canadian Journal of Chemical Engineering*, *70*, 786–793.

Elnashaie, S. S. E. H., & Alhabdan, F. M. (1989). Mathematical modelling and computer simulation of industrial water-gas shift converters. *Mathematical and Computer Modelling*, *12*, 1017–1034.

Elnashaie, S. S. E. H., & Elshishini, S. S. (1993). *Modelling, simulation and optimization of industrial catalytic fixed bed reactors*. Amsterdam: Gordon and Breach.

Ettouney, H. M., Shaban, H. I., & Nayfeh, L. J. (1993). Theoretical analysis of high and low temperature shift converters. *Transactions of the Institute of Chemical Engineers, Part A*, *71*, 189–195.

Hawker, P. N. (1982). Shift CO plus steam to H_2. *Hydrocarbon Processing*, *61,* 183–187.

Kul'kova, N. V., & Temkin, M. I. (1949). *Zhurnal Fizicheskoi Khimii*, *23*, 695–702.

Kumar, R. (1994). Pressure swing adsorption process: Performance optimum and adsorbent selection. *Industrial and Engineering Chemistry Research*, *33*, 1600–1605.

Kumar, R., Fox, V. G., Hartzog, D. G., Larson, R. E., Chen, Y. C., Houghton, P. A., & Nahein, T. (1994). A versatile process simulator for adsorptive separations. *Chemical Engineering Science*, *49*, 3115–3125.

Malek, A. (1996). *A study of H_2 purification from the refinery fuel gas by pressure swing adsorption.* Ph.D. thesis, National University of Singapore.

Oki, S., & Mezaki, R. (1973). *Journal of Physical Chemistry*, *77*, 1601–1608.

Rajesh, J. K., Gupta, S. K., Rangaiah, G. P., & Ray, A. K. (2000). Multiobjective optimization of steam reformer performance using genetic algorithm. *Industrial and Engineering Chemistry Research*, *39*, 706–717.

Rase, H. F. (1977). *Chemical reactor design for process plants,* vol. 2. New York: Wiley.

Ruthven, D. M. (1969). The activity of commercial water-gas shift catalysts. *Canadian Journal of Chemical Engineering*, *47*, 327–331.

Shahani, G. H., Garodz, L. J., Murphy, K. J., Baade, W. F., & Sharma, P. (1998). Hydrogen and utility supply optimization. *Hydrocarbon Processing*, *77,* 143–150.

Singh, C. P. P., & Saraf, D. N. (1977). Simulation of high-temperature water-gas shift reactors. *Industrial Engineering Chemistry, Process Design and Development*, *16*, 313–319.

Singh, C. P. P., & Saraf, D. N. (1979). Simulation of side fired steam-hydrocarbon reformers. *Industrial Engineering Chemistry, Process Design and Development*, *18*, 1–7.

Srinivas, N., & Deb, K. (1995). Multiobjective function optimization using nondominated sorting genetic algorithms. *Evolutionary Computation*, *2*, 221–248.

Wolf, D., Barré-Chassonnery, M., Höhenberger, M., van Veen, A., & Baerns, M. (1998). Kinetic study of the water-gas shift reaction and its role in the conversion of methane to syngas over a Pt/Mgo catalyst. *Catalysis Today*, *40*, 147–156.

Xu, J., & Froment, G. F. (1989a). Methane steam reforming, methanation and water-gas shift: I. Intrinsic kinetics. *American Institute of Chemical Engineers Journal*, *35*, 88–96.

Xu, J., & Froment, G. F. (1989b). Methane steam reforming: II. Diffusional limitations and reactor simulation. *American Institute of Chemical Engineers Journal*, *35*, 97–103.

Xue, E., O'Keeffe, M., & Ross, J. R. H. (1996). Water-gas shift conversion using a feed with a low steam to carbon monoxide ratio and containing sulphur. *Catalysis Today*, *30*, 107–118.